THE JOURNAL OF PHYSICAL CHEMISTRY

Caltech Library

Subscriber access provided by Caltech Library

C: Surfaces, Interfaces, Porous Materials, and Catalysis

Probing Surface Chemistry at an Atomic Level; Decomposition of 1-Propanethiol on GaP(001)(2×4) Investigated by STM, XPS, and DFT

Seokmin Jeon, Minho Kim, Peter W. Doak, Harry A Atwater, and Hyungjun Kim

J. Phys. Chem. C, **Just Accepted Manuscript** • DOI: 10.1021/acs.jpcc.8b10993 • Publication Date (Web): 04 Jan 2019

Probing Surface Chemistry at an Atomic Level; Decomposition of 1-Propanethiol on GaP(001)(2×4) Investigated by STM, XPS, and DFT

Seokmin Jeon,[1,*,‡] *Minho Kim,*[2,‡] *Peter W. Doak,*[3] *Harry A. Atwater,*[1] *and Hyungjun Kim*[2,*]

[1]Thomas J. Watson Laboratories of Applied Physics, California Institute of Technology, MC 128-95, Pasadena, California 91125, USA

[2]Department of Chemistry, Korea Advanced Institute of Science and Technology (KAIST), 291 Daehak-Ro, Yuseong-Gu, Daejeon 34141, Korea

[3]Computational Science & Engineering Division and Center for Nanophase Materials Sciences, Oak Ridge National Laboratory, Oak Ridge, Tennessee 37831, USA

ABSTRACT

The adsorption and decomposition mechanisms for 1-propanethiol on a Ga-rich GaP(001)(2×4) surface are investigated at an atomic level using scanning tunneling microscopy (STM), X-ray photoelectron spectroscopy (XPS) and density functional theory (DFT) calculations. Using a combination of experimental and theoretical tools, we probe the detailed structures and energetics of a series of reaction intermediates in the thermal decomposition pathway from 130 to 773 K. At 130 K, the propanethiolate adsorbates are observed at the edge gallium sites, with the thiolate-Ga bonding configuration maintained up to 473 K. Further decomposition produces two new surface features, Ga-S-Ga and P-propyl species at 573 K. Finally, S-induced (1×1) and (2×1) reconstructions are observed at 673 ~ 773 K, which are reportedly associated with arrays of surface Ga-S-Ga bonds and subsurface diffusion of S. To understand the observed site-selectivity on the hydrogen dissociation of the thiol molecule at 130 K, the two most likely dissociation pathways (Ga-P *vs.* Ga-Ga dimer sites) are investigated using DFT Gibbs energy calculations. While the theory predicts the kinetic advantage for the dissociation reaction occurring on the Ga-P dimer (Lewis acid-base combination), we only observed dissociation products on the Ga-Ga dimer (Lewis acid). The DFT calculations clarify that the reversible thiolate diffusion along the Ga dimer row prevents recombinative desorption, which is probable on the Ga-P dimer. Together with experimental and theoretical results, we suggest a thermal decomposition mechanism for the thiol molecule with atomic-level structural details.

1. INTRODUCTION

Organic thin films have attracted growing interest due to their multifunctionality towards chemical modification and physical/electronic protection afforded to various types of inorganic solid surfaces.[1-4] For instance, organic films can improve electronic and optoelectronic properties of semiconductors by passivating the mid-gap trap states and lifting electronic band edge pinning.[5]

III-V semiconductors are promising materials in many device applications including photovoltaics, light emitting diodes (LEDs), and light sensors due to their high carrier mobility and direct/wide band gap.[6] Alkanethiols are suitable materials for use as protective adlayers on III-V semiconductor surfaces because of multiple advantages: 1) the sulfur head group enables the organic molecules to strongly graft onto the inorganic surface via metal-sulfur bonds, 2) the sulfur atom electronically passivates the surface mid-gap states, and 3) the organo-sulfur molecules offer chemical flexibility to the inorganic surface by functionalizing the organic tail groups. It is useful to understand the detailed structure and energetics of the organosulfur molecules on the III-V semiconductor surfaces at an atomic level especially for fabrication and control of sub-nanoscale devices such as molecular or quantum devices.

There are a few studies that have investigated the mechanisms for dissociative adsorption of H_2S[7] and short-chain alkanethiols[8-10] on III-V semiconductors using X-ray photoelectron spectroscopy (XPS) and temperature-programmed desorption (TPD), both of which measure the ensemble properties of the molecule. Real-space observations of the local structures have been limited to elemental sulfur-induced surface reconstructions.[11] However, no report has observed single-molecule-resolved details for the adsorption and decomposition reactions of alkanethiols on a III-V semiconductor surface. Furthermore, most previous theoretical works[12-16] on the structures and energetics of dissociatively adsorbed organosulfur molecules on III-V semiconductor surfaces

have provided limited support by spectroscopic measurements, which do not capture the detailed local chemistry between the single adsorbate molecule and the surface atoms.

In this study, we use scanning tunneling microscopy (STM), XPS and density functional theory (DFT) calculations to investigate the adsorption and decomposition reactions of 1-propanethiol molecules on a Ga-rich GaP(001)(2×4) surface. The combination of these three powerful techniques enables us to elucidate the atomic structures and reaction thermodynamics of a single organic molecule adsorbed on a well-defined model surface.

2. EXPERIMENTAL AND COMPUTATIONAL METHODS

2.1. Experimental Details

Sample preparation. A GaP(001) wafer (*n*-type, carrier concentration 1.7×10^{18} cm^{-3}, EL-CAT Inc.) was cleaved and mounted onto a tantalum sample plate using two tantalum foils, and then loaded into an ultra-high vacuum (UHV) sample preparation chamber (base pressure < 1×10^{-10} Torr). The GaP(001) sample surface was cleaned by several cycles of sputtering with 500 eV Ne^+ ions for 7 minutes at 523 K and annealing at 773 K for 10 minutes in the preparation chamber. Sample temperature was measured using the type-K thermocouples located near the heaters in STM and XPS systems. Due to the designs of the sample holders and the heaters, there possibly exist offsets between the temperature measured by the thermocouples and the actual sample temperature. We expect that the actual sample temperature could be lower than the measured temperatures by 19 ~ 32 K at 573 K and 40 ~ 55 K at 773 K based on the tests conducted using Si wafers and an optical pyrometer (See Section 1 in Supporting Information for details).

After preparing a clean surface in the preparation chamber, it was transferred under vacuum to the STM analysis chamber (base pressure < 3×10^{-11} Torr). The Ga-rich GaP(001)(2×4) mixed-

dimer reconstruction was reliably prepared using the sputtering-annealing method, with no other reconstruction structure observed.[11,17,18]

1-Propanethiol (99 %, Aldrich) was purchased and further purified via several freeze-pump-thaw cycles to remove dissolved gases prior to exposure to the GaP sample. The source chemical was inserted into the STM chamber using a variable leak valve at 298 K. The amount of dosing is expressed in Langmuir (1 Langmuir (L) = 1×10^{-6} Torr·s). The temperature of the sample surface during dosing was 130 K if otherwise noted, which was measured using a Si diode sensor.

STM experiment. The STM characterization of the surface topography was carried out using a commercial STM (VT-STM XA 50/500, Omicron Nanotechnology) and electrochemically etched tungsten tips. The filled-state STM images were obtained in a constant current mode with the sample bias voltage varied from –3.5 V ~ –4.5 V and a set-point current of 100 ~ 200 pA. Low-temperature STM images were obtained at 130 K for the surface that had been exposed to the molecular source at 130 K. For annealing experiments, the molecule pre-dosed sample was transferred to the preparation chamber and warmed up to 298 K. The analysis chamber was also warmed up to 298 K. After warming up, the sample was sent back to the analysis chamber for characterization at 298 K. For higher temperature annealing, the sample was transferred to the preparation chamber and heated up to a target annealing temperature (573 ~ 673 K) with a ramping rate of 1 K/s, and then held at this temperature for 30 minutes. All the STM images except for the low-temperature images were taken at 298 K after appropriate warming or cooling.

XPS experiment. X-ray photoelectron spectroscopy (XPS) measurements were carried out in a separate UHV chamber (base pressure, $< 3 \times 10^{-9}$ Torr), which is located in the Beckman Institute, California Institute of Technology, Pasadena, USA. The system is equipped with a Kratos Ultra DLD spectrometer and monochromatic Al Kα radiation ($h\nu$ = 1486.58 eV) source. 1-

Propanethiol was dosed on the clean GaP(001)(2×4) surfaces at 298 K in the sample preparation chamber of the UHV-STM system. The as-dosed samples were transferred to the XPS system using a portable stainless steel chamber filled with anhydrous nitrogen gas, which minimizes exposure to ambient gas during transportation. XP spectra were obtained at room temperature from either as-transferred or annealed samples at 573 ~ 773 K for 30 minutes with a ramping rate of 1 K/s in the UHV-XPS chamber. Low-resolution survey and high-resolution spectra were collected at fixed analyzer pass energies of 80 and 10 eV, respectively. The spectra were collected at 45° with respect to the surface normal direction. The binding energies of the spectra were referenced to the clean Au $4f_{7/2}$ core level spectrum with a fixed binding energy of 84.0 eV. The XPS data were analyzed with commercial software, CasaXPS (version 2.3.16). The individual peaks were fitted with a Gaussian/Lorentzian product function after a Shirley background subtraction. Spin-orbit splittings and branching ratios were held constant; 1.1 eV and 0.51 for the S 2*p* core level, 0.86 eV and 0.52 for the P 2*p* core level, and 0.44 eV and 0.69 for the Ga 3*d* core level, respectively.[19]

The substrate-overlayer model[20] was used to calculate the coverage of the surface-adsorbed molecules and sulfur atoms from the XPS core-level spectroscopic data (See Section 2 in Supporting Information for details).

2.2. Computational Details.

Two surface modeling approaches were employed for understanding detailed adsorption structures and the reaction energetics; the slab model and the cluster model approaches. The slab model approach was used to figure out the adsorbate conformation dependency on energy as well as the ground state structure calculations for STM simulation. The calculations were carried out using the Perdew-Burke-Ernzerhof (PBE) exchange-correlation functional[21] with the projector-

augmented wave (PAW) pseudopotentials[22,23] and its van der Waals-corrected methods such as Grimme's D3 method[24] as implemented in the Vienna Ab initio Software Package program (VASP).[25-28] The kinetic energy cutoff for plane wave and the Monkhorst-Pack k-mesh were set to be 380 eV and 4×2×1 for the slab model, respectively, as described in our previous report[29]. The geometry was optimized until energy difference of the last two steps becomes 1.0×10^{-4} eV. During geometry optimizations, the two layers at the bottom of a slab were fixed while the top five layers and the adsorbates were fully relaxed. STM simulation images were produced within the Tersoff-Hamann theory using the band-decomposed partial charge analysis in VASP[30,31].

To understand the dissociation mechanism for the adsorbed 1-propanethiol on the GaP(001)(2×4) surface, we employed the cluster model approach in which a finite $Ga_{25}P_{21}H_{30}$ cluster structure was used, as shown in Figure 1(d). A significant number of probable reaction intermediates in the dissociation pathways were investigated using both periodic and cluster models. We found no difference in the relative adsorption energies between the two methods. The cluster model was calculated using Becke's three-parameter nonlocal-exchange functional[32] with the correlation functional of Lee-Yang-Parr[33] (B3LYP[34]) as implemented in the Jaguar 8.4 software package.[35] For the calculation of the cluster model, we employed the LACVP** basis set, which describes a gallium atom using the LANL2DZ effective core potential[36] and the remaining atoms using the 6-31G basis set.

The cluster model consists of one Ga-P dimer in the first layer and four Ga-Ga dimers in the second layer.[18] The Ga and P atoms below the second level were constructed to maintain four covalent networks on each atom using H atoms and lone pairs of electrons. The number of H atoms was carefully chosen to satisfy the electron counting model.[37] Thereby, the P atom in the first layer has one completely filled dangling bond (two electrons in the non-bonding orbital), and each of

the five sp^2 Ga atoms on the first and second layers has an empty dangling bond (no electron in the non-bonding orbital). All structures were fully optimized until the maximum elements of gradient and nuclear displacement become 4.5×10^{-4} hartree/bohr and 1.8×10^{-3} bohr, respectively, and the energy difference between the last two optimization steps becomes 5.0×10^{-5} hartree without geometrical constraints on any atom in the cluster model.

3. RESULTS AND DISCUSSION

3.1. Structure analysis by STM and DFT calculations

Figure 1 shows the constant-current STM images obtained from the clean GaP surfaces consisting of Ga-rich GaP(001)(2×4) mixed-dimer surface reconstruction. In a filled-state image (negative sample bias voltage), an atomic terrace is observed that is composed of alternating bright and dark rows running along the $[\bar{1}10]$ direction, which are called dimer and vacancy rows, respectively. In higher magnification images, one can resolve an array of bright protrusions in the dimer row. Each protrusion on the dimer is assigned to the lone pair electrons of the P atom in the 1st layer Ga-P dimer of the (2×4) unit cell (1P in Figure 1d). The apparent shape of the (2×4) cell in STM images depends on the sample bias voltage, as shown in Figure 1b. At –4.5 V, the lone pair electrons in the 1st layer P are dominant in both experimental and simulated STM images. At –2.5 V, two less-bright protrusions whose locations are overlapped with the two Ga-Ga back bonds (2Ga-6Ga in Figure 1d) are better resolved. The energies and spatial charge distributions of the P lone pair and the Ga back bond electrons in the filled-state STM images are also consistent with those of the two highest occupied bands (similar to the highest occupied molecular orbitals, HOMO) of the surface reconstruction.[18]

Special care is needed when analyzing the STM images of the clean Ga-rich GaP(001)(2×4) surface based on the known (2×4) mixed-dimer surface reconstruction model. In the high-resolution STM images, we found that the distance between the neighboring protrusions along $[\bar{1}10]$ is not constant due to variation in the directions of the Ga-P dimers with respect to their neighboring dimers (Figure 1c). Two types of surface defects were commonly observed on the clean surfaces; a point defect and a line defect (see insets in Figure 1a). These defects are associated with the misfit adsorptions of the 1st or 2nd layer Ga-P and Ga-Ga dimers on top of the (1×1) lattice of the 3rd layer P atoms. The point defect (left inset in Figure 1a) is formed by the occupation of more than one 1st layer of Ga-P dimers in a (2×4) cell. The line defect (right inset in Figure 1a) is also called a domain boundary (DB), which stems from a fault alignment of two dimer rows approaching from the two opposite directions along $[\bar{1}10]$. Those defects could play a role in the diffusion barriers for adsorbate molecules, which move along the dimer rows. Details for such diffusion will be explained in the theory section below.

Figure 2 exhibits the constant-current STM images of 1-propanethiol/GaP(001)(2×4) at various coverages and temperatures. At 130 K, bright protrusions (feature A) are observed in-between dimer rows (or in the vacancy row) as a result of the adsorption of 1-propanethiol molecules onto the clean surface. Another feature of the surface at this temperature is that each molecule is placed at a random location of the surface due to the lack of diffusion and aggregation at low temperature.

The STM image in Figure 2b was obtained after annealing the sample in Figure 2a to 298 K. The feature B at 298 K is substantially larger and ~0.6 Å taller than the feature A at 130 K (comparing the insets in Figure 2a and b). The apparent diameter of the protrusion of feature B is comparable to double the edge length of the (1×1) unit cell, which is 7.71 Å, as shown in Figure

3b. Since the molecular length of 1-propanethiol in the gas phase was estimated to be 4.18 Å from the S atom to the terminal C atom in our B3LYP calculation, the diameter of feature B is comparable to double the molecular chain length of the 1-propanethiol molecule. However, the adsorption location of the molecule with respect to the surface atoms is barely changed. Most of the adsorbates are no longer isolated from each other but instead form aggregations of multiple molecules. The adsorbate density is especially higher around the atomic step edges and the DB, which is associated with the interruption of adsorbate diffusion.

We further investigated the detailed adsorption structures for the dissociated reaction products by comparing the experimental and simulated STM images. A nucleophilic chalcogenide molecule favorably forms a Ga-chalcogenide bond after H dissociation on the Ga-rich GaP(001)(2×4) surface.[29] Low-temperature synchrotron photoemission spectroscopy studies also showed that the H atom of H_2S or the alkanethiol molecule dissociates at 100 ~ 105 K to form S-metal bonds on InP and GaAs(001) surfaces.[7,10] Based on previous DFT studies,[38,39] there are two potential adsorption sites for the dissociated H atom; one site is on the 1P atom (H-1P bond) and the other is located on the edge Ga-Ga dimers (Ga-H-Ga bond). The location of the center of the bright protrusion in Figure 3a is consistent with the S atom when the propanethiolate adsorbate is bound to the edge Ga atom (3Ga or 4Ga in Figure 1d). Four adsorption conformations have been found in DFT calculations (Figure S1 in Supporting Information), with the geometry of the most stable conformation based on van der Waals corrected DFT energy calculations is proposed to represent feature A, as exhibited in Figure 3a.

To figure out the adsorption structure of feature B, we compare the experimental STM images with the DFT-STM simulation images. Since we found that the center locations of the bright protrusions for feature A and B are the same, we postulate that the bond between the

molecule and the surface atom is maintained. Based on a van der Waals corrected DFT method (PBE-D3), the rotational barrier over the lowest three conformations of the propanethiolate bound to the edge Ga atom is 15 meV, which can be overcome at the measurement temperature of 298 K. The stark difference in the apparent shapes for feature A and B in the STM images is, therefore, proposed to result from rotation of the Ga-S bond. The synthesized STM simulation image, which is obtained by superposing the STM simulation images of the four propanethiolate conformations, is consistent with the apparent shapes of feature B in the STM images (Figure 3b).

On the surface that was annealed at 573 K, two new features are observed in the STM images (C and D in Figure 2c). Feature C has a symmetry against the mirror plane halving the (2×4) unit cell, so the adsorbate is bound to the atom located on the middle line of the dimer row (1P or 2Ga), as shown in Figure 3c. The less bright feature (feature D), on the other hand, is located near the 2nd layer Ga-Ga dimers (called an edge Ga dimer), as shown in Figure 3d. The large apparent size of feature C is associated with rotation of the P-C bond of the surface propyl adsorbate.

Lastly, the other new features (E and F) are observed when further annealing the sample at 673 K, as shown in Figure 2d. Feature E in Figure 2d is composed of small protrusions with (1×1) or (2×1) symmetry whose apparent height is ~0.8 Å lower than the first layer P atom. Emergence of the (2×1) and (1×1) surface reconstructions at high coverage S on InP(001) and GaAs(001) surfaces has been extensively studied by low energy electron diffraction (LEED), XPS, and STM.[40-43] Based on previous research, this feature is associated with subsurface diffusion and P-substitution by the dissociated S atoms. In contrast to feature E, the apparent shape of feature F is irregular with a lack of periodicity and ~0.5 Å higher than the first layer P atom in the STM images. As opposed to feature B in Figure 2b, feature F shows a larger distribution in size, and the

adsorption location is hardly defined with respect to the lattice of the surface atoms (incommensurate adsorption). We propose that this feature is attributed to the Ga-P clusters as a result of combination of the surface Ga and the subsurface P that was substituted by S. This is supported by the XPS data, which will be shown in the following section, since there is no significant change in the Ga 3*d* or P 2*p* XPS spectra as a function of annealing temperature at 298 ~ 773 K, indicating maintenance of Ga-P bond character and exclusion of the formation of elemental Ga, P, or S clusters.

3.2. Chemical bonding characterization by XPS

Figure 4 and Table 1 show S 2*p* and C 1*s* core-level XPS spectra for the GaP(001)(2×4) surface that was exposed to 1-propanethiol at 298 K followed by annealing to various temperatures. The presented S 2*p* spectra were obtained by subtracting the Ga 3*s* spectrum of the clean GaP(001)(2×4) surface whose peak is located approximately 160.2 eV from the S 2*p*/Ga 3*s* regions, which showed the variation of the S 2*p* spectral features more clearly. This procedure is justified because the relative intensity and spectral shape of the Ga 3*s* peak and the Ga 3*d* peak are nearly constant over the samples with various coverages and temperatures (refer to Figure S2 in Supporting Information).

The S 2*p* region is fitted with three discrete components throughout the annealing temperatures of interest (blue, magenta, and green plots in Figure 4a). The S 2*p* core-level spectrum at 298 K is fitted with a single component (Ga-S in blue) whose binding energy is highest among all the components. Due to the difference in the electronegativity between S (2.6) and Ga (1.8), the S 2*p* binding energy decreases as the strength and/or number of bonds increases between Ga and S. The Ga-S component, which is dominant at 298 K, has the lowest interaction with the

surface Ga.

The Ga-S-Ga component (magenta in Figure 4a), which emerges at 573 K, has the lowest binding energy among all the components (–1.8 eV *vs.* Ga-S) due to the strongest interaction between S and Ga. Interestingly, the S coverage at 573 K is similar to that at 298 K, as shown in Table 1. On the other hand, the carbon coverage drops to 60 % as the sample is heated. Thus, the dominant surface reaction from 298 to 573 K is expected to be the dissociation of the S-C bond and desorption of hydrocarbon species, leaving S on the surface. This observation is consistent with the STM data in which we observe a much higher coverage for feature D compared to feature C in Figure 2c.

In Figure 4a, the S 2*p* spectrum obtained from the sample annealed at 773 K shows a green component (Subsurface S) as well as the magenta component (Ga-S-Ga). This green component has a binding energy that lies in-between the two low-temperature components, Ga-S-Ga and Ga-S. These observations are consistent with the results in previous reports[40-43] where XPS studies showed that Ga-S-Ga and diffused subsurface S coexist in the S-treated III-V surfaces annealed at similar temperatures. The reported binding energy shift due to the subsurface diffusion with respect to the Ga-S-Ga state is +0.4 ~ 1.0 eV, which agrees with our observation, +0.7 eV. In our STM data, we observed (1×1) and (2×1) reconstructions at 673 ~ 773 K (Figure 2d). The surface reconstructions are therefore associated with arrays of Ga-S-Ga on the surface and diffused S atoms underneath the surface.

In Table 1, the XPS data indicate a significant decrease in carbon coverage from 0.19 to 0.07 ML when the sample annealing temperature is increased from 573 to 773 K. This decrease represents desorption of the surface bound propyl group.[8,10] The trace amount of carbon left after annealing at 773 K is difficult to identify in our experiments since a comparable amount of

adventitious carbon contaminant was detected after relocating samples between two UHV systems (More discussion is in Section 5, Supporting Information).

In contrast to the S 2*p* and C 1*s* regions, no significant variation was found in the Ga 3*d* and P 2*p* regions (Figure S2 in Supporting Information). Based on our DFT calculations, up to 3 molecules can exist for every 9 surface Ga atoms or 1 surface P atom in a (2×4) unit cell. However, there are more intense XPS signals coming from the bulk Ga and P atoms because a photoelectron kinetic energy of larger than 1000 eV can escape at least 10 layers of surface and bulk Ga and P atoms. Therefore, it is difficult to resolve the behavior of the surface Ga without a surface sensitive setup such as synchrotron-radiation XPS with small kinetic energy and high photoelectron ejection angle.

3.3. Reaction thermodynamics by DFT calculations

Figure 5 summarizes the Gibbs free energy diagram at 130 K and 573 K for possible dissociation pathways of a 1-propanethiol molecule on a GaP(001)(2×4) cluster model. It is notable that there is a kinetic preference for the dissociation of thiol at the Ga atom of the Ga-P mixed dimer site in the 1st layer (+8.32 kcal/mol at the 2Ga site versus +19.19 kcal/mol at the 3Ga site and +18.28 kcal/mol at the 4Ga site at 130 K), which is not observed in the STM data, where the thiol dissociation occurs at the edge Ga dimer site (3Ga-5Ga or 4Ga-6Ga in Figure 1d). One possible explanation for this inconsistency is that a much lower activation barrier for the reverse reaction of the thiol dissociation at the Ga atom of the mixed dimer site (+26.44 kcal/mol at 2Ga site versus +41.00 kcal/mol at 3Ga site and +37.25 kcal/mol at 4Ga site) leads to recombinative desorption of propanethiolate and the hydrogen atom at the 2Ga site. Further analysis on the dissociation of dipropyl disulfide also reveals that the kinetic barrier for recombination in the

reverse reaction at the edge Ga site (+35.16 kcal/mol) is 13.02 kcal/mol higher than that at the Ga atom of the mixed dimer site (+22.14 kcal/mol), as shown in Figure S4. As temperature increases from 130 K to 573 K, we observed sharp increase of adsorption barrier and mild increase of dissociation kinetic barrier in both propanethiol and dipropyl disulfide, indicating that the initial adsorption and dissociation of a thiol occur at low temperature range.

In contrast to the recombinative desorption at the 2Ga site, the propanethiolate species at the edge Ga sites (3Ga and 4Ga site) suffer from barrier-less alkylate diffusion, as shown in Figure 6. The thermodynamic energy difference is only a few orders of kcal/mol (2.06 kcal/mol), which indicates that the alkylthiolate diffusion is highly reversible compared to the thiol dissociation reactions. Mulliken charge analysis shows that the two gallium atoms along the 4Ga-8P-3Ga chain make a major contribution to the charge transfer from the GaP surface to the propanethiolate adsorbate [δq_{4Ga} = +0.052 and δq_{3Ga} = +0.044 vs. δq_{ProSH} = –0.28 in the case of structure (5-1); δq_{3Ga} = +0.058 and δq_{4Ga} = +0.046 vs. δq_{ProSH} = –0.28 in the case of structure (5-3)], indicating that both Ga atoms are in equivalently electron-deficient states, which leads to the reversible diffusion of propanethiolate along the Ga atoms at the short-edge side with a low thermodynamic barrier.

IV. CONCLUSION

We have investigated the atom specific local geometries and reaction energetics for a 1-propanethiol molecule adsorbed onto a GaP(001)(2×4) surface using STM and XPS experiments and DFT calculations. The STM observations at 130 K reveal that the propanethiolate species are initially adsorbed at the edge Ga sites. From commensurate experimental observations based on the DFT results, it is concluded that (1) the thiolate species adsorbed at the 1st layer Ga-P dimer

site suffers from recombinative desorption, while (2) the diffusion of thiolate species along the Ga-P-Ga chain at the vacancy row prevents recombinative desorption of the thiolate adsorbed at the edge Ga site of the vacancy row. Temperature-dependent STM and XPS studies further reveal that the decomposition mechanism for thiolate under various temperature regimes occurs as follows:

$$\text{Propanethiolate} - \text{Ga}_{\text{edge}}(a) + \text{Ga} - \text{H} - \text{Ga}_{\text{edge}}(a), \quad 130\ \text{K} \sim 473\ \text{K}$$

$$\text{Propyl} - \text{P}_{\text{top}}(a) + \text{Ga} - \text{S} - \text{Ga}_{\text{edge}}(a), \quad 573\ \text{K}$$

$$\text{S}(1 \times 1)\ or\ \text{S}(2 \times 1)(a) + \text{Ga} - \text{P aggregation}\ (a), \quad 673\ \text{K} \sim 773\ \text{K}$$

where (a) implies the adsorbate state at the GaP surface. Our observation provides a sub-molecular level of understanding for the thermal decomposition pathways of organosulfur molecules based on experiments and simulations. This work will also grant an opportunity for beneficial improvement of III-V semiconductor surfaces with organic passivation and functionalization.

ASSOCIATED CONTENT

The Supporting Information is available free of charge on the ACS Publications website.

Section 1: Temperature offsets between two measurements methods; thermocouples *vs.* optical pyrometer.

Section 2: Substrate-overlayer model for the estimation of coverage.

Section 3: DFT adsorption energies of various conformations of propanethiolate-Ga (Figure S1).

Section 4: Temperature-dependent XPS in the Ga 3*d* and P 2*p* regions (Figure S2).

Section 5: Analysis of adventitious carbon contamination while transferring samples from UHV-STM to UHV-XPS systems (Figure S3).

Section 6: DFT thermodynamics of disulfide bond dissociation of dipropyldisulfide (Figure S4)

AUTHOR INFORMATION

Corresponding Author

*E-mail: seokmin.jeon.ctr.ks@nrl.navy.mil (S.J.) and linus16@kaist.ac.kr (H.K.)

Present Addresses

[1]National Research Council Research Associateship Program, U.S. Naval Research Laboratory, Washington, DC 20375, United States

Author Contributions

STM and XPS experiments were carried out by S.J. DFT calculations were carried out by M.K, H.K. and S.J. The manuscript was written through contributions of all authors. STM simulations were done by P.D. and S.J. ‡These authors contributed equally.

Notes

The authors declare no competing financial interest.

ACKNOWLEDGMENT

This work was supported by Department of Energy. S.J. thanks to Kwanjeong Educational Foundation for support. XPS measurement was carried out in the Molecular Materials Research Center of the Beckman Institute of Caltech. S.J. thanks Liangbo Liang at CNMS, Oak Ridge National Laboratory for sharing the STM simulation code that he developed. M.K. and H.K. acknowledges the support by the Global Frontier R&D Program (2013M3A6B1078884) and the Creative Materials Discovery Program (Grant 2017M3D1A1039378) granted through the National Research Foundation of Korea (NRF).

REFERENCES

(1) Dubowski, J. J.; Voznyy, O.; Marshall, G. M. Molecular Self-Assembly and Passivation of GaAs (001) with Alkanethiol Monolayers: A View towards Bio-Functionalization. *Appl. Surf. Sci.* **2010**, *256*, 5714−5721.

(2) Srisombat, L.; Jamison, A. C.; Lee, T. R. Stability: A Key Issue for Self-Assembled Monolayers on Gold as Thin-Film Coatings and Nanoparticle Protectants. *Colloids and Surfaces A: Physicochem. Eng. Aspects* **2011**, *390*, 1-19.

(3) Kim, J. –S.; Yoo, H. –W.; Choi, H. O.; Jung, H. –T. Tunable Volatile Organic Compounds Sensor by Using Thiolated Ligand Conjugation on MoS_2. *Nano Lett.* **2014**, *14*, 5941-5947.

(4) Pearce, B. L.; Wilkins, S. J.; Paskova, T.; Ivanisevic, A. A Review of In Situ Surface Functionalization of Gallium Nitride via Beaker Wet Chemistry. *J. Mater. Res.* **2015**, *30*, 2859-2870.

(5) Sheldon, M. T.; Eisler, C. N.; Atwater, H. A. GaAs Passivation with Trioctylphosphine Sulfide for Enhanced Solar Cell Efficiency and Durability. *Adv. Energy Mater.* **2012**, *2*, 339–344.

(6) Del Alamo, J. A. Nanometre-Scale Electronics with III-V Compound Semiconductors. *Nature* **2011**, *479*, 317-323.

(7) Hung, W. –H.; Chen, H. –C.; Chang, C. –C.; Hsieh, J. –T.; Hwang, H. –L. Adsorption and Decomposition of H_2S on InP(100). *J. Phys. Chem. B* **1999**, *103*, 3663-3668.

(8) Donev, S.; Brack, N.; Paris, N. J.; Pigram, P. J.; Singh, N. K.; Usher, B. F. Surface Reactions of 1-Propanethiol on GaAs(100). *Langmuir* **2005**, *21*, 1866-1874.

(9) Flores-Perez, R.; Zemlyanov, D. Y.; Ivanisevic, A. Quantitative Evaluation of Covalently Bound Molecules on GaP (100) Surfaces. *J. Phys. Chem. C* **2008**, *112*, 2147-2155.

(10) Huang, T. P.; Lin, T. H.; Teng, T. F.; Lai, Y. H.; Hung, W. H. Adsorption and Thermal Reaction of Short-Chain Alkanethiols on GaAs(100). *Surf. Sci.* **2009**, *603*, 1244-1252.

(11) Sanada, N.; Shimomura, M.; Fukuda, Y.; Sato, T. Clean GaP(001)-(4×2) and H_2S-Treated (1×2)S Surface Structures Studied by Scanning Tunneling Microscopy. *Appl. Phys. Lett.* **1998**, *67*, 1432-1434.

(12) Lu, H. –L.; Chen, W.; Ding, S. –J.; Xu, M.; Zhang, D. W.; Wang, L. –K. Quantum Chemical Study of Adsorption and Dissociation of H_2S on the Gallium-Rich GaAs(001)-4×2 Surface. *J. Phys. Chem. B* **2006**, *110*, 9529-9533.

(13) Voznyy, O.; Dubowski, J. J. Structure, Bonding Nature, and Binding Energy of Alkanethiolate on As-Rich GaAs (001) Surface: A Density Functional Theory Study. *J. Phys. Chem. B* **2006**, *110*, 23619-23622.

(14) Voznyy, O.; Dubowski, J. J. Adsorption Kinetics of Hydrogen Sulfide and Thiols on GaAs (001) Surfaces in a Vacuum. *J. Phys. Chem. C* **2008**, *112*, 3726-3733

(15) Tang, S.; Cao, Z. Density Functional Characterization of Adsorption and Decomposition of 1-Propanethiol on the Ga-Rich GaAs (001) Surface. *J. Phys. Chem. A* **2009**, *113*, 5685-5690.

(16) Gao, W.; Zhu, S. E.; Zhao, M. Methylthiolate Adsorbed on As-Rich GaAs (001) Surface. *J. Mater. Sci.* **2011**, *46*, 1021-1026.

(17) Lüdge, K.; Vogt, P.; Pulci, O.; Esser, N.; Bechstedt, F.; Richter, W. Clarification of the GaP(001)(2×4) Ga-Rich Reconstruction by Scanning Tunneling Microscopy and Ab Initio Theory. *Phys. Rev. B* **2000**, *62*, 11046-11049.

(18) Schmidt, W. G. III-V Compound Semiconductor (001) Surfaces. *Appl. Phys. A* **2002**, *75*, 89-99.

(19) Suzuki, Y.; Sanada, N.; Shimomura, M.; Fukuda, Y. High-Resolution XPS Analysis of GaP(001), (111)A, and (111)B Surfaces Passivated by $(NH_4)_2S_x$ Solution. *Appl. Surf. Sci.* **2004**, *235*, 260-266.

(20) Briggs, D.; Seah, M. P. *Practical Surface Analysis: Auger and X-ray Photoelectron Spectroscopy*; 2nd ed.; Wiley: New York, 1990.

(21) Perdew, J. P.; Burke, K.; Ernzerhof, M. Generalized Gradient Approximation Made Simple *Phys. Rev. Lett.* **1996**, *77*, 3865– 3868.

(22) Blöchl, P. E. Projector Augmented-Wave Method. *Phys. Rev. B* **1994**, *50*, 17953-17979.

(23) Kresse, G.; Joubert, D. From Ultrasoft Pseudopotentials to the Projector Augmented-Wave Method. *Phys. Rev. B* **1999**, *59*, 1758-1775.

(24) Grimme, S.; Antony, J.; Ehrlich, S.; Krieg, H. A Consistent and Accurate Ab Initio Parametrization of Density Functional Dispersion Correction (DFT-D) for the 94 Elements H-Pu *J. Chem. Phys.* **2010**, *132*, 154104.

(25) Kresse, G.; Hafner, J. Ab Initio Molecular Dynamics for Open-Shell Transition Metals. *Phys. Rev. B* **1993**, *48*, 13115-13118.

(26) Kresse, G.; Hafner, J. Ab Initio Molecular-Dynamics Simulation of the Liquid-Metal-Amorphous-Semiconductor Transition in Germanium. *Phys. Rev. B* **1994**, *49*, 14251-14269.

(27) Kresse, G.; Furthmüller, J. Efficiency of Ab-Initio Total Energy Calculations for Metals and Semiconductors Using a Plane-Wave Basis Set. *Comput. Mater. Sci.* **1996**, *6*, 15-50.

(28) Kresse, G.; Furthmüller, J. Efficient Iterative Schemes for Ab Initio Total-Energy Calculations Using a Plane-Wave Basis Set. *Phys. Rev. B* **1996**, *54*, 11169-11186.

(29) Jeon, S.; Kim, H.; Goddard, W. A.; Atwater, H. A. DFT Study of Water Adsorption and Decomposition on a Ga-Rich GaP(001)(2×4) Surface. *J. Phys. Chem. C* **2012**, *116*, 17604-17612.

(30) Tersoff, J.; Hamann, D. R. Theory and Application for the Scanning Tunneling Microscope. *Phys. Rev. Lett.* **1983**, *50*, 1998-2001.

(31) Tersoff, J.; Hamann, D. R. Theory of the Scanning Tunneling Microscope. *Phys. Rev. B* **1985**, *31*, 805-813.

(32) Becke, A. D. Density-Functional Thermochemistry. III. The Role of Exact Exchange. *J. Chem. Phys.* **1993**, *98*, 5648-5652.

(33) Lee, C.; Yang, W.; Parr, R. G. Development of the Colle-Salvetti Correlation-Energy Formula into a Functional of the Electron Density. *Phys. Rev. B* **1988**, *37*, 785-289.

(34) Stephens, P. J.; Devlin, F. J.; Chabalowski, C. F.; Frisch, M. J. Ab Initio Calculation of Vibrational Absorption and Circular Dichroism Spectra Using Density Functional Force Fields. *J. Phys. Chem.* **1994**, *98*, 11623-11627.

(35) Bochevarov, A. D.; Harder, E.; Hughes, T. F.; Greenwood, J. R.; Braden, D. A.; Philipp, D. M.; Rinaldo, D.; Halls, M. D.; Zhang, J.; Friesner, R. A. Jaguar: A High-Performance Quantum Chemistry Software Program with Strengths in Life and Materials Sciences. *Int. J. Quantum Chem.* **2013**, *113*, 2110-2142.

(36) Hay, P. J.; Wadt, W. R. Ab Initio Effective Core Potentials for Molecular Calculations. Potentials for K to Au Including the Outermost Core Orbitals. *J. Chem. Phys.* **1985**, *82*, 299-310.

(37) Pashley, M. D. Electron Counting Model and Its Application to Island Structures on Molecular-Beam Epitaxy Grown GaAs(001) and ZnSe(001). *Phys. Rev. B* **1989**, *40*, 10481-10487.

(38) Woo, R. L.; Das, U.; Cheng, S. F.; Chen, G.; Raghavachari, K.; Hicks, R. F. Phosphine and Tertiarybutylphosphine Adsorption on the Indium-Rich InP (001)-(2×4) Surface. *Surf. Sci.* **2006**, *600*, 4888-4895.

(39) Das, U.; Raghavachari, K.; Woo, R. L.; Hicks, R. F. Phosphine Adsorption on the In-Rich InP(001) Surface: Evidence of Surface Dative Bonds at Room Temperature. *Langmuir* **2007**, *23*, 10109-10115.

(40) Shimomura, M.; Naka, K.; Sanada, N.; Suzuki, Y.; Fukuda, Y.; Mo, P. J. Surface Structures and Electronic States of H_2S-Treated InP (001). *J. Appl. Phys*. **1996**, *79*, 4193-4196.

(41) Shimomura, M.; Sanada, N.; Ichikawa, S.; Fukuda, Y.; Nagoshi, M.; Møller, P. J. Surface Reconstruction of InP(001) upon Adsorption of H_2S Studied by Low-Energy Electron Diffraction, Scanning Tunneling Microscopy, High-Resolution Electron Energy Loss, and X-Ray Photoelectron Spectroscopies. *J. Appl. Phys*. **1998**, *83*, 3071-3076.

(42) Moriarty, P.; Murphy, B.; Roberts, L.; Cafolla, A. A.; Hughes, G.; Koenders, L.; Bailey, P. Photoelectron Core-Level Spectroscopy and Scanning-Tunneling-Microscopy Study of the Sulfur-Treated GaAs (100) Surface. *Phys. Rev. B* **1994**, *50*, 14237-14245.

(43) Preobrajenskia, A.B.; Gebhardta, R.K.; Uhliga, I.; Chassé, T. Two Types of Sulfur-Induced (2×1) Reconstructions on InP(001). *Surf. Sci*. **2001**, *481*, 1-12.

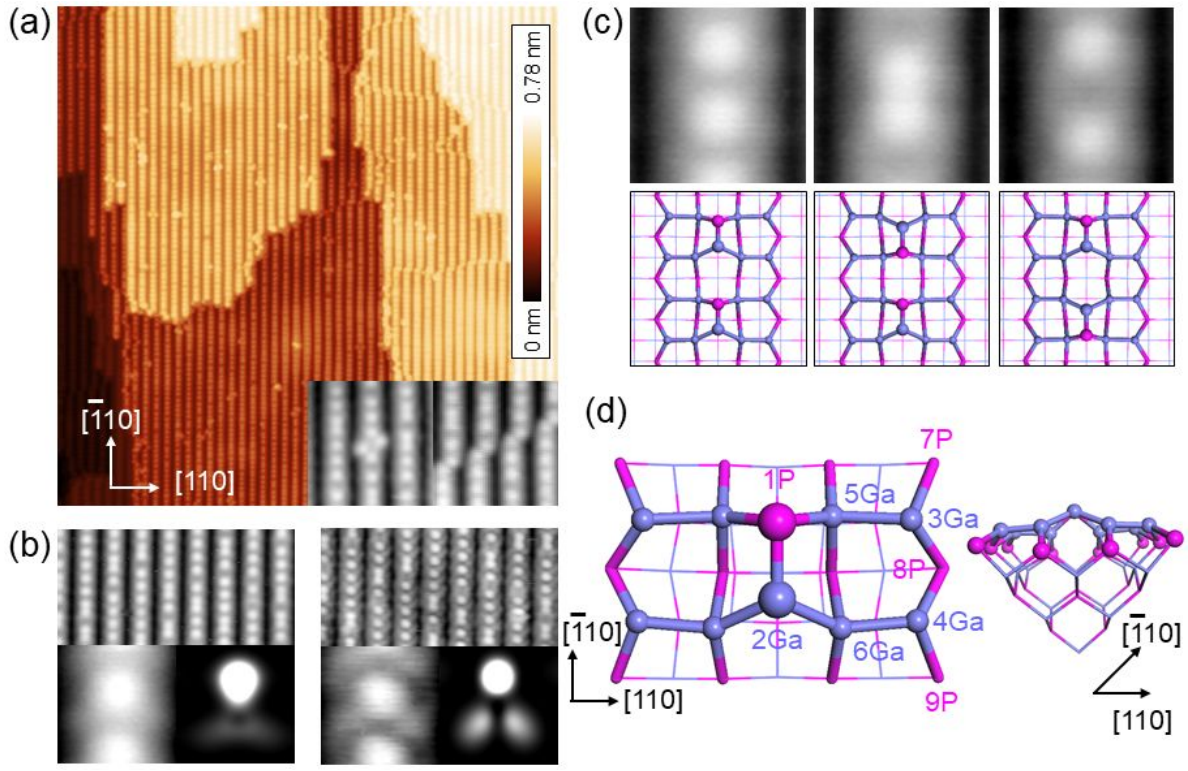

Figure 1. A clean GaP(001)(4×2) mixed-dimer surface reconstruction. a) Constant-current STM image (V_s = –4.5 V; It = 150 pA, image size 80 nm^2). Insets in a) display two representative defects (left: point defect, right: domain boundary "DB" defects). b) Voltage-dependency for the STM images (left: –4.5 V, 200 pA, right: –2.5 V, 200 pA, image size 15 nm^2). Insets of each image in b) show zoom-in (left) and simulated (right) STM images. The sample voltages of the simulated images are –2.3 V (left) and –0.5 V(right) from the valence band maximum. c) Three configurations of neighboring Ga-P dimers; (top row) STM images (V_s = –4 V; It = 200 pA, image size: 2 nm^2) and (bottom row) their structure models. d) The top (left) and the front (right) views of a $Ga_{25}P_{21}H_{30}$ cluster model. Magenta and violet spheres represent Ga and P atoms.

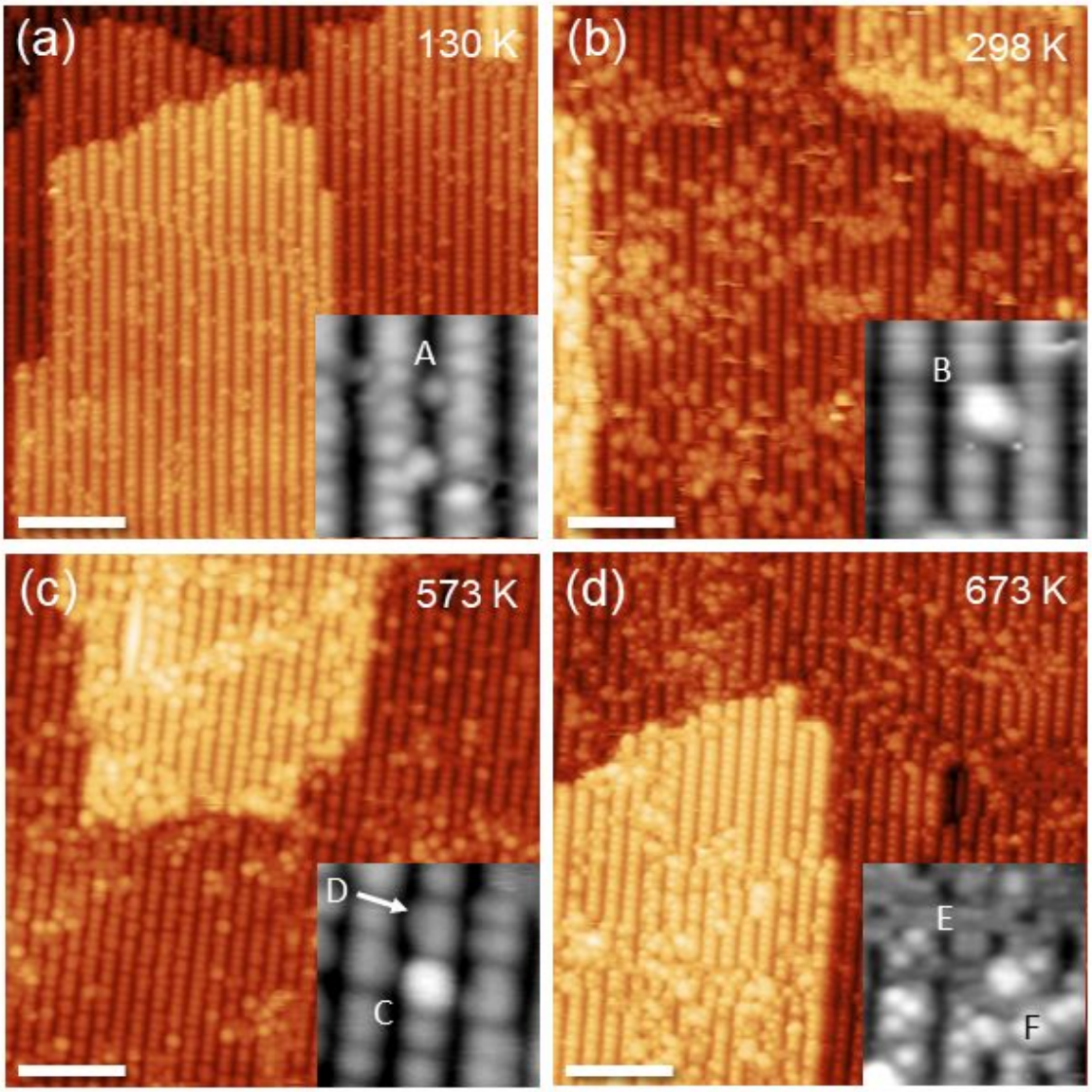

Figure 2. Thermal decomposition of 1-propanethiol on GaP(001)(2×4). a) Constant-current STM image of the clean surface exposed to 0.005 L 1-propanethiol at 130 K. b) A clean GaP(001)(2×4) is exposed to 0.02 L 1-propanethiol at 130 K followed by annealing at 298 K. c) The sample in b) is annealed at c) 573 K and d) 673 K for 30 minutes, respectively. Image a) was obtained at 130 K, and b) to d) were obtained at RT. The size of the scale bars is 10 nm. Tunneling parameters for all the STM images; $V_s = -4.5$ V; $I_t = 100\sim150$ pA.

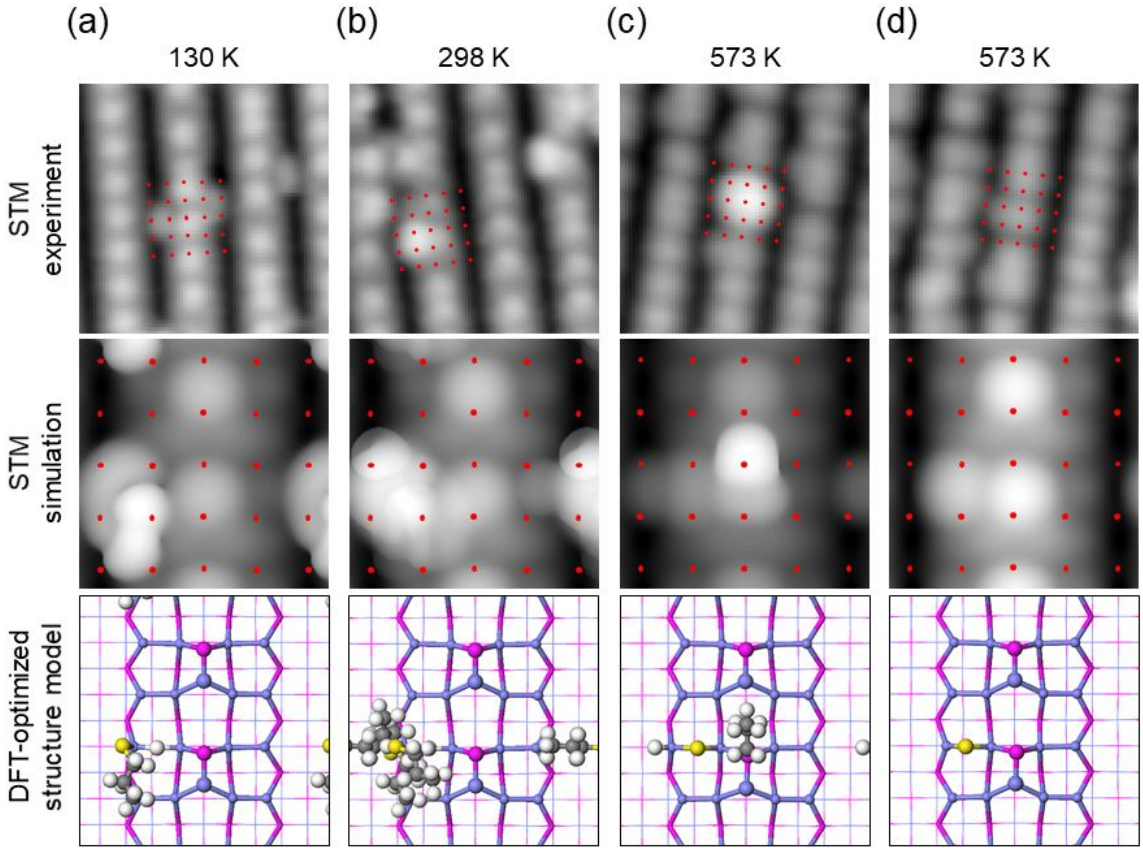

Figure 3. From top to bottom, experimental and simulated STM images (V_s = –4.5 V; I_t = 100~150 pA) and the DFT-optimized structure models for the dissociated adsorbates of propanethiol/GaP(001) at various temperatures. The simulated STM image and the structure model in b) are created by overlapping the four calculated ground state models (Section 3 in Supporting Information). All simulated STM images are obtained at –3 eV from the valence band maximum. The grids of red dots represent the (1×1) surface unit cells, which are overlaid on both the experimental and simulated STM images.

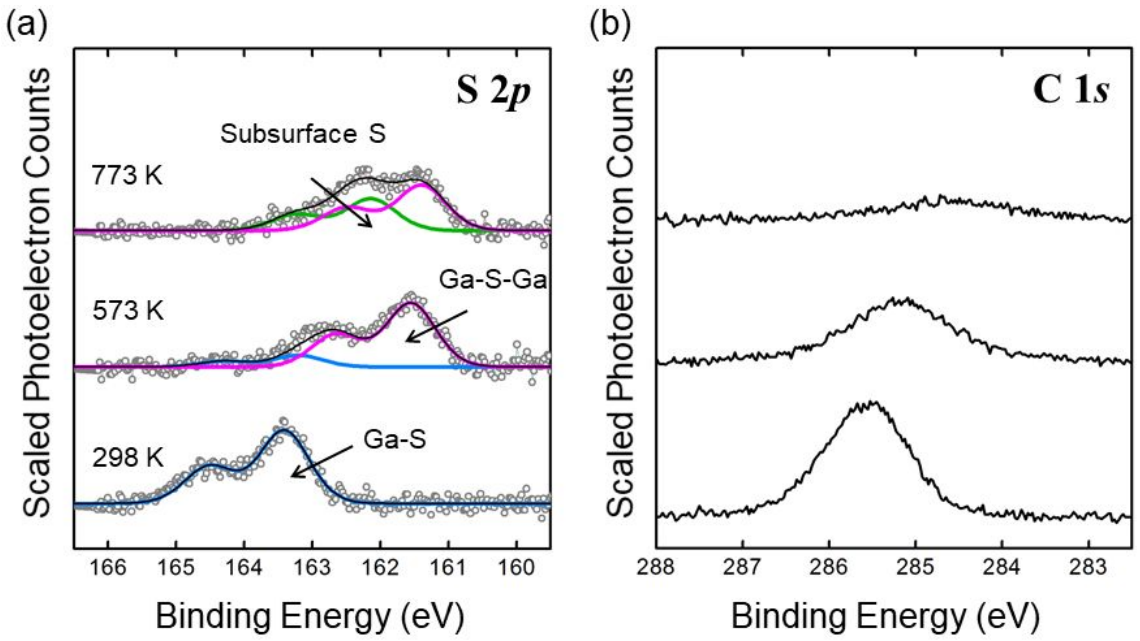

Figure 4. S 2*p* and C 1*s* X-ray photoelectron spectra of 1-propanethiol/GaP(001). A clean GaP(001)(2×4) surface is exposed to 1×10^4 L 1-propanethiol and followed by annealing at the displayed temperatures for 30 minutes before measurements at 298 K. In a), the Ga 3*s* peak (160.2 eV) of the clean GaP(001)(2×4) was subtracted to show only the S 2*p* spectra. Blue, magenta, and green components in the S *2p* region are assigned to Ga-S, Ga-S-Ga, and subsurface S, respectively.

Experiment	Ga $3d_{5/2}$		S $2p_{3/2}$ (Ga-S)		S $2p_{3/2}$ (Ga-S-Ga)		S $2p_{3/2}$ (Subsurface S)		C 1s		Coverage (ML)	
	position (eV)	area* (count)	position (eV)	area* (count)	position (eV)	area* (count)	position (eV)	area* (count)	position (eV)	area* (count)	Sulfur	Carbon
298 K	19.51	2548	163.4	162.0					285.6	946	0.07	0.32
573 K	19.46	2582	163.2	23.1	161.6	125.9			285.2	578	0.06	0.19
773 K	19.37	2870			161.4	86.9	162.1	61.1	284.6	237	0.06	0.07

Table 1. Tabulated S 2*p* X-ray photoelectron spectra deconvolution and coverage calculation results for the 1-propanethihol/GaP(001) samples in Figure 4.

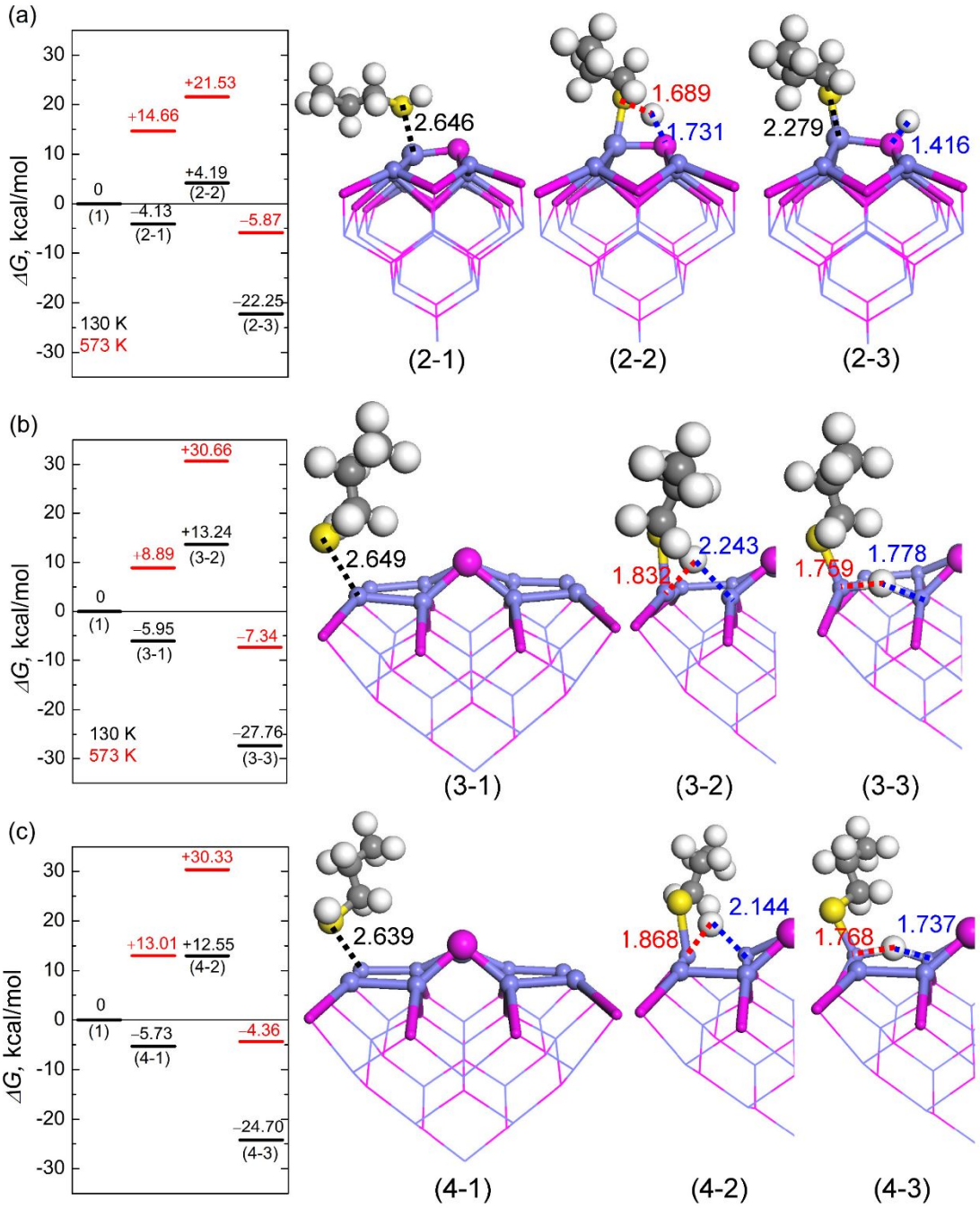

Figure 5. (left) DFT calculated reaction free energies at 130 K in black and 573 K in red and (right) optimized structures for the 1-propanethiol adsorption and dissociation pathways on the top (a) 2Ga site and the edge (b) 3Ga and (c) 4Ga sites of the $Ga_{25}P_{21}H_{30}$ cluster. Numbers in parentheses in the energy diagrams are the corresponding structure numbers. The adsorbed complex before dissociation (left), transition state for the dissociation (middle), and the complex after thiol dissociation (right). White for hydrogen, yellow for sulfur, gray for carbon, magenta for phosphorus, and violet for gallium. Hydrogen atoms at the truncation of the cluster for charge balance are not shown for simplicity. The atoms on the first two layers are highlighted by a ball-and-stick model. The numbers in the structures denote the distance in Å.

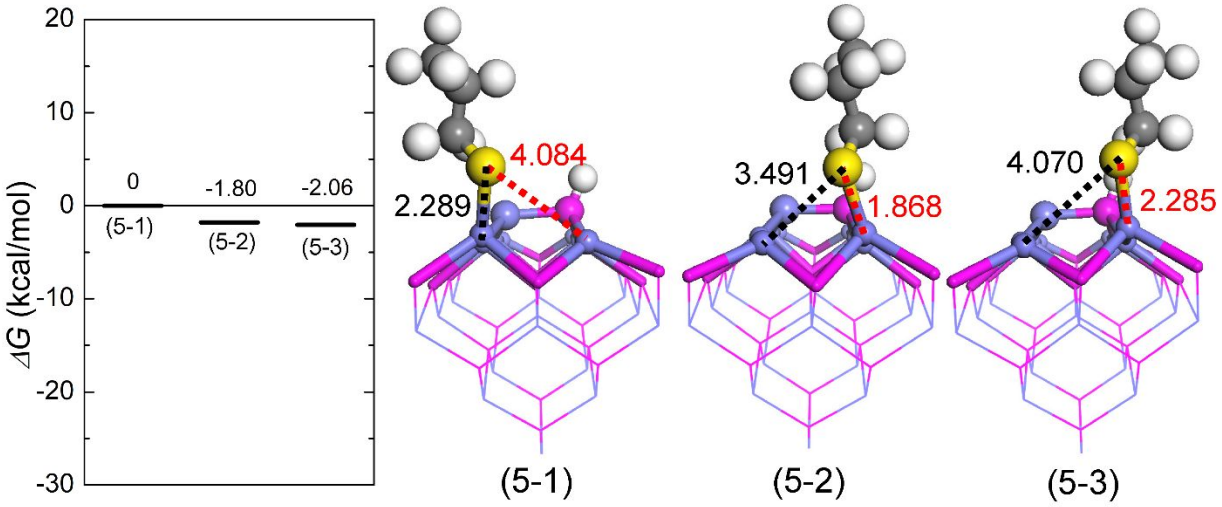

Figure 6. (left) DFT calculated reaction free energies at 130 K and (right) optimized structures for the diffusion of propanethiolate along the short-edge gallium sites. Numbers in parentheses in the energy diagrams are the corresponding structure numbers. White for hydrogen, yellow for sulfur, gray for carbon, magenta for phosphorus, and violet for gallium. Hydrogen atoms at the truncation of the cluster for charge balance are not shown for simplicity. The atoms at the first two layers are highlighted as a ball-and-stick model. The numbers below the structures denote the distance in Å.

TOC Graphic